

Templated Fabrication of Fiber-Basket Polymersomes via Crystallization-Driven Block Copolymer Self-Assembly

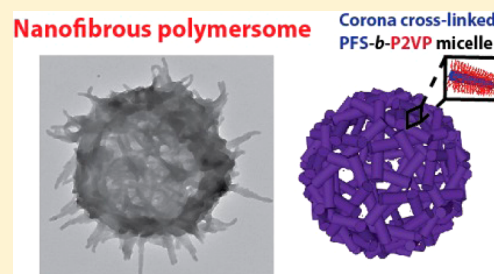
Lin Jia,[†] Lemuel Tong,[†] Yi Liang,[†] Amy Petretic,[†] Gerald Guerin,^{*,†} Ian Manners,^{*,†} and Mitchell A. Winnik^{*,†}

[†]Department of Chemistry, University of Toronto, 80 St. George Street, Toronto, Ontario M5S 3H6, Canada

[‡]School of Chemistry, University of Bristol, Bristol BS8 1TS, U.K.

Supporting Information

ABSTRACT: Immobilizing uniform nanostructures on a mesoscale substrate is a promising approach to prepare nanometer to micrometer sized materials with new functionalities. The hierarchical structures formed depend on both the nature of the substrate and the components deposited. In this paper, we describe the use of colloidal polystyrene microbeads as a sacrificial template to create a nanofibrous network coating consisting of elongated block copolymer micelles. This network has a secondary structure very different from that of conformal coatings obtained by other methods. In addition, the fibers of the network could be elongated by crystallization-driven self-assembly. The network was locked in place by cross-linking the micelles through in situ generation of small Pt nanoparticles. Subsequent removal of the sacrificial template gave an open vesicular structure. To demonstrate further transformation of the membrane, we showed that the cross-linked micelles could also be used to embed silver nanoparticles. The sacrificial template contained known amounts of Tb and Tm ions, allowing us to estimate via atomic mass spectrometry that 85% of the template surface was covered with micelle seeds. This approach to fabricating hierarchical coating structures expands the generality and scope of template-assisted synthesis to build advanced hierarchical materials with precise morphological control.



INTRODUCTION

Materials with complex and multidimensional hierarchical structures often exhibit unique functions and attractive properties. Such materials play an important role in nanotechnology.^{1–3} One of the objectives of contemporary bottom-up self-assembly is the development of methodologies for the creation of colloidal structures of controlled shape, uniform in size, that incorporate both complexity and hierarchy into the design.^{4–10} One effective approach to preparing nanostructured materials is templated synthesis that involves a sequence of steps including (i) preparation of the template, (ii) directed synthesis of the target material using the template, and (iii) removal of the template if necessary.¹¹

Many authors have reported templated syntheses using dispersions of inorganic nanoparticles^{7,9} or microparticles^{12–14} as rigid templates. Soft templates such as emulsion droplets,¹⁵ microemulsions,¹⁶ micelles^{17–20} and vesicles²¹ were also used to obtain templated coatings. Most of these reports have focused on obtaining uniform conformal coatings²² through a sol–gel approach,^{23–25} layer-by-layer noncovalent interactions²⁶ and graft-polymerization reactions.^{27–29} For many of these syntheses, removal of the template by dissolution or thermolytic decomposition (calcination) afterward led to stable hollow structures.^{13,14,24}

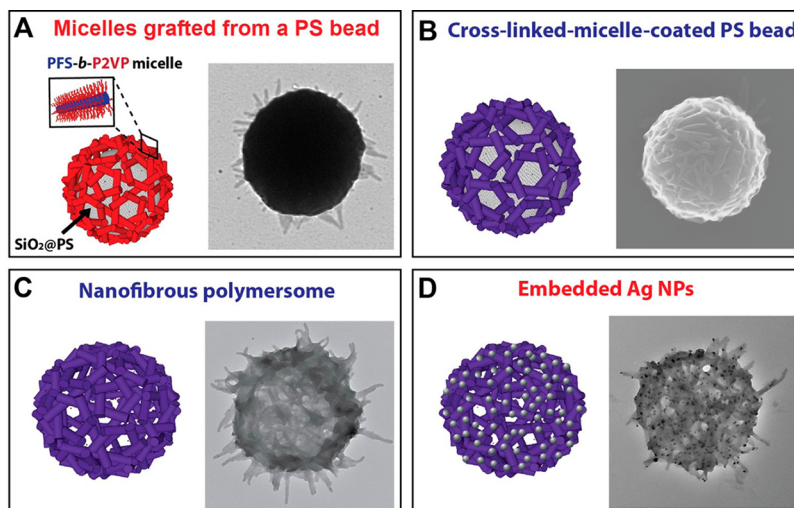
Instead of uniform conformal structures, we are interested in hierarchical coatings with secondary structure, for example, nanofibrous layers on a template, as well as the hollow basket-

like structures that result from removing the template. Two examples in the literature caught our attention.^{28,30} The hierarchy of these nanofibrous structures in both types of materials made them suitable for a number of unique applications. Jiang et al.²⁸ reported the preparation of PS microparticles coated with a network of polyaniline (PANI) nanofibers by the polymerization of aniline from the particle surface. The PANI-coated particles were much easier to process than PANI itself. The convolutions on the template made films of the particles superhydrophobic and also highly conducting (0.5 S/cm). The second example, reported by Liu et al.,³⁰ involved poly(L-lactide) (PLLA) nanofibrous hollow microspheres with a relatively broad size distribution. They were obtained through an emulsion process, followed by quenching the mixture in liquid nitrogen to induce phase separation, resulting in the formation of nanofibers at the surface of the emulsion droplets. The nanofibrous PLLA hollow microspheres were able to accommodate chondrocyte cells and enhance cartilage regeneration in an ectopic implantation mode in animal models.

We want to expand the library of hierarchical structures that can be obtained by bottom-up self-assembly. As a step in this direction, we recently reported a “grafting-from” strategy to grow stiff elongated block copolymer (BCP) micelles from the

Received: September 29, 2014

Published: November 18, 2014

Scheme 1. Protocol to Prepare the Hollow Hierarchical Nanofibrous Assemblies^a

^a(A) The mesoscale hierarchical structures with short micelles (PFS₃₀-*b*-P2VP₃₀₀) growing from SiO₂@PS template through the “seeded growth” strategy. (B) The P2VP corona in the hierarchical structure in (A) was cross-linked by addition of Karstedt’s catalyst and 1,1,3,3-tetramethyldisiloxane (TMDS) in 2-PrOH. (C) The hollow hierarchical nanofibrous assemblies were obtained by removal of PS beads in DCM. (D) Generation of Ag NPs in the PFS-*b*-P2VP micelles of the nanofibrous assemblies via an in situ reduction of Ag⁺ ions by the Fe(II) moieties of the swollen redox-active PFS core in DCM.

surface of inorganic nanoparticles or nanorods as the structural template.³¹ The novel feature of this strategy is that the micelles were grown by living crystallization-driven self-assembly (CDSA) from initiating crystallites attached to the template surface.^{32–40} This process is a nanoscale analogue of a “growing-from” living polymerization of individual polymer molecules from initiators attached to a surface. The specific examples reported involved polyferrocenyldimethylsilane-*block*-poly(2-vinylpyridine) (PFS-*b*-P2VP) as the crystalline-coil block copolymer, 2-propanol (2-PrOH) as the selective solvent, and silica nanoparticles or silica-coated nickel hydrazine nanorods as the central structural feature.³¹

In this paper, we describe a multistep template-assisted approach to fabricate nanofibrous hollow structures. Starting from silica coated polystyrene microbeads as the template, we attached block copolymer crystallites (PFS-*b*-P2VP micelle seeds) to the surface. The PS beads contained a known amount of Tb and Tm ions, an important factor for quantifying the subsequent steps in the templated synthesis. As summarized in Scheme 1, these colloiddally stable multicomponent particles initiate the living growth of uniform cylindrical micelles from their surface, and the size and shape of the resulting three-dimensional hierarchical structures can be precisely controlled via CDSA. Through subsequent steps of corona cross-linking and removal of the template, uniform nanofibrous hollow hierarchical structures were obtained. Structures of greater complexity can be further obtained by generating silver nanoparticles (Ag NPs) in the micelle, taking advantage of the redox-activity of the ferrocene units in the crystalline core.

RESULTS AND DISCUSSION

Creating the Template for Bead-Micelle Assemblies.

As templates, we employed a sample of poly(*N*-vinylpyrrolidone) (PVP)-coated PS beads originally prepared for mass cytometry measurements.^{41,42} These particles, with a number-average diameter of $d_n = 1.19 \mu\text{m}$ ($d_w/d_n = 1.04$, d_w is the weight-average diameter, Figure S1) were synthesized by a

two-stage dispersion polymerization that included PVP as the polymeric stabilizer. Methacrylic acid (MAA, 2 wt %), TbCl₃·6H₂O, and TmCl₃·6H₂O (1 wt % each, all based on styrene) were added in the second stage. Details are provided in the Supporting Information (Experimental Section). By titration, the particles contained on average 1.6×10^7 MAA groups per bead, corresponding to ca. 6 –COOH groups per nm². This value is slightly higher than the 4 –COOH groups per nm² characteristic of carboxylated PS particles prepared by emulsion polymerization.⁴³

As seed-crystallite micelles, we employed a sample of PFS₃₀-*b*-P2VP₃₀₀ (where the subscripts refer to the number-average degrees of polymerization). Long micelles were prepared by heating a sample of PFS₃₀-*b*-P2VP₃₀₀ in 2-PrOH to 90 °C for 30 min followed by cooling to room temperature as described previously.³¹ This sample was subjected to mild sonication to obtain a dispersion of micelle fragments (mean length $L_n = 179$ nm, $L_w/L_n = 1.04$; L_n , number-average length; L_w , weight-average length) that were characterized by transmission electron microscopy (TEM, Figure S2a). Initially, we anticipated that the pyridine groups comprising the P2VP corona on the micelle fragments dispersed in 2-PrOH would bind to the –COOH groups on the PS particle surface, but this interaction turned out to be ineffective. It is likely that the solvent-swollen polyvinylpyrrolidone corona on the PS particles restricted close approach of the BCP seed crystallites to the particle surface. As a consequence, we chose to coat the PS beads with a thin layer of silica (SiO₂@PS, Figure S2b,c, see Supporting Information). The polyvinylpyrrolidone corona promotes the local deposition of the silica,¹² which, under our conditions, formed a rough layer consisting of silica nanoparticles. The purified SiO₂@PS was characterized by thermogravimetric analysis (TGA, Figure S3a) to determine the weight fraction of coated silica.

To prepare the seed coated SiO₂@PS, an aliquot of PFS-*b*-P2VP seed crystallites in 2-PrOH (0.5 mg, 1 mL) was mixed with an aqueous suspension of SiO₂@PS (1.5 mg, 1 mL) and allowed to age for 24 h. The excess crystallites in solution were

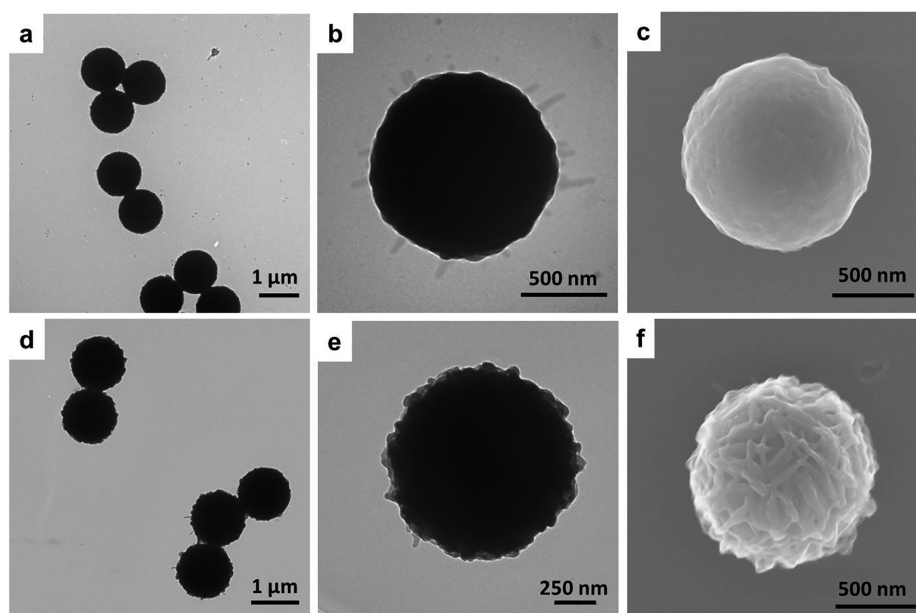


Figure 1. (a,b) TEM and (c) SEM images of PS-micelle assemblies with short protruding micelles prepared by addition of PFS₃₀-*b*-P2VP₃₀₀ in THF (2.5 μL, 10 mg mL⁻¹) to 2-PrOH (1 mL) containing seed coated SiO₂@PS (0.15 mg mL⁻¹) and aged 24 h. (d,e) TEM and (f) SEM images of corona cross-linked PS hybrid assemblies with short protruding micelles (from structures in (a–c)) in 2-PrOH. In the text and in the Supporting Information, the terms **1c** and **1f** refer to the samples whose structures are shown in (c) and (f), respectively.

then removed by sedimentation followed by redispersion of the PS particles in fresh 2-PrOH solvent. The TEM image in Figure S2d shows the purified seed coated SiO₂@PS. It is important to note that the seed coated particles are colloidally stable. The presence of the micelle seed fragments was difficult to discern on the surface of the seed coated SiO₂@PS particles in either TEM or SEM images (Figure S2d,e,f). However, analysis of the seed coated SiO₂@PS particles by energy dispersive X-ray (EDX) spectroscopy showed strong signals of iron demonstrating that the seeds were in fact present (Figure S4).³¹

To determine the mean number of seeds per PS bead, we carried out inductively coupled plasma atomic emission spectroscopy (ICP-AES) measurements on the PS beads and the seed coated PS beads after microwave digestion. Both samples contained lanthanide ions (Tb and Tm) from the particle synthesis, and the latter sample contained iron from the PFS-*b*-P2VP micelle seeds. The concentrations of Tb and Tm in the PS beads were measured by the peak area under the respective wavelengths 350.917 and 313.126 nm. We obtained a 1 to 1 ratio of Tb (0.18 ± 0.003 ppm) and Tm (0.18 ± 0.003 ppm). The mass of lanthanide per bead (2.0 μg per bead, 0.03 wt %) was calculated with eq S1. For the analysis of the data for the PFS₃₀-*b*-P2VP₃₀₀ seed coated beads, we took the signal of Tm as a reference to compare with the iron signal. The concentrations of Fe and Tm obtained were 0.310 ± 0.002 ppm and 0.061 ± 0.001 ppm, respectively. On the basis of the ratio of Fe to Tm (ca. 5) and the degree of polymerization of the PFS block (DP = 30) in PFS₃₀-*b*-P2VP₃₀₀, we obtained 7.1 × 10⁵ polymer molecules per PS bead. We know the mean length of the micelle seeds ($L_n = 179$ nm), and assume that these micelles have the same linear aggregation number (4 chains per nm) as the PFS₂₃-*b*-P2VP₂₃₀ sample that we studied previously.⁴⁴ In this way, we calculate that there were ca. 700 micelle seeds per bead. To estimate the surface coverage of the PS beads, we assumed that the micelle seeds lay flat on the bead surface. If the average area of a seed is approximated by a

rectangle with dimensions of 179 × 30 nm, we calculate (eq S2) that about 85% of the surface area of the PS beads was covered by the seeds.

Directed Self-Assembly on the Bead Template. Seeded Growth. To test the effectiveness of the seed coated SiO₂@PS for seeded growth of elongated core-crystalline micelles, a suspension of these beads in 2-PrOH was treated with an aliquot of PFS₃₀-*b*-P2VP₃₀₀ unimer in tetrahydrofuran (THF). After brief swirling, the mixture was set aside to age for 24 h, leading to spherical structures with a rough surface (Figure 1a,b,c). A TEM image at higher magnification (Figure 1b) shows protrusions from the edge of a PS particle with lengths up to 200 nm. These appear to be short PFS-*b*-P2VP micelles. Because of the large diameter of the PS microbead, it was difficult to obtain a good focus on the protruding micelles. We can, however, estimate the total length of the micelles ($L_{n,expected}$) with eq 1.

$$L_{n,expected} = \left(\frac{m_{unimer}}{m_{seeds}} + 1 \right) L_{n,seeds} \quad (1)$$

This expression combines the average length of micelle seeds ($L_{n,seeds}$) on the surface of the template with the weight of unimer added into the solution, m_{unimer} , and that of the seeds anchored on the polystyrene beads, m_{seeds} . If we assume that all of these seeds were active for micelle growth, we calculate a value of $L_{n,expected} = 1030$ nm, close to the diameter of the PS beads (1200 nm).

Cross-Linking the Corona. The key step toward formation of an interconnected network of nanofibers on the surface of the PS template is the cross-linking of the P2VP corona chains of the micelles. We began with a sample of PFS-*b*-P2VP micelles@SiO₂@PS in 2-PrOH shown in the SEM image in Figure 1c. For convenience, we refer to this sample as **1c**. We followed the approach of Qiu et al.⁴⁵ by cross-linking the corona of the PFS-*b*-P2VP micelles with Pt nanoparticles (NPs) which are formed by the addition of Karstedt's catalyst, a

labile Pt(0) complex, in the presence of 1,1,3,3-tetramethyldisiloxane (TMDS). The TEM and SEM images in Figure 1d,e,f show the product of corona cross-linking for **1c** after the sample was aged for 24 h at room temperature. We refer to these corona cross-linked structures as **1f**. Interestingly, **1f** reveals a different surface morphology compared to **1c**. In sample **1f** the network of fiber-like micelles on the surface of the template can be clearly distinguished. We infer that the morphological change of the surface was due to the formation of the cross-linked corona. The cross-linking process adds the mass, volume, and the enhanced electron density of the Pt cross-linker to the P2VP chains. The local shape changes associated with binding these Pt NPs lead to the walnut-like texture of the PS microbead surface. More information on the cross-linked structures is available from EDX analysis: samples of **1c** and **1f** (Figure S5 and S6) showed strong signals from iron. More important is that sample **1f** also showed strong signals from platinum.

Removing the Template: Hollow Fiber-Basket Mesostructures. To remove the template from the mesostructures, we used DCM at room temperature to dissolve the PS.⁴⁶ The corona cross-linked sample **1f** was first collected by centrifugation (5000 rpm/5 min), and then separated from the dissolved PS by three cycles of sedimentation–resuspension in DCM. The sample was finally dispersed in 2-PrOH, with the idea that the selective solvent would lead to resolidification of the PFS component. An aliquot of each colloidal solution was analyzed by electron microscopy and by EDX. TEM images in Figure 2a,b and Figure S7 show the structures after removal of the PS template from **1f**. We refer to the structures in Figure 2b as **2b**.

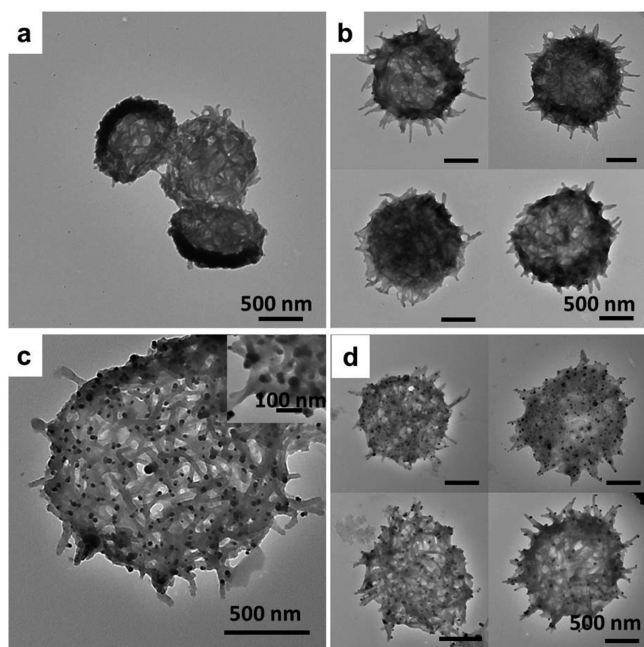


Figure 2. (a,b) TEM images of the nanofibrous hollow structures after removal of PS beads from corona cross-linked structures **1f** by sedimentation–resuspension in DCM. In the text and Supporting Information, the term **2b** refers to the samples whose structures are shown in (b). (c,d) TEM images of Ag NPs embedded in the framework of the hollow structures of **2b** from different positions of the same grid at different magnifications.

The structures in Figure 2b appear to be hemispherical caps consisting of a thin membrane of fibrous material. One can clearly see the individual PFS-*b*-P2VP micelles in the interwoven network that forms the external membrane. We believe that these structures were formed by collapse of the membrane after removal of the PS template. The edges of the structures appear to have a higher contrast compared to the center. In addition, the number-average diameter of **2b** ($d_n = 1.36 \mu\text{m}$) was ca. 170 nm larger than that of **1f** ($d_n = 1.19 \mu\text{m}$). These observations are also consistent with the collapse of hollow structures in solution upon drying on the TEM grid.

It is well-known that hollow structures with thin membranes formed by soft matter often collapse while drying for characterization by TEM.^{26,47,48} Maintaining the three-dimensional structure is dependent on the rigidity of the material, the thickness of the membrane, and the size of the structure.^{30,49} We infer that without the support of the PS beads, the hollow fiber-basket structures collapsed to form the hemispherical disk-like shapes of **2b** when they were dried on the TEM grid. One can see that the cross-linked micelle fibers formed a relatively thin membrane surrounding the template. Use of DCM to remove the core PS bead also caused dissolution of the PFS micelle core, destroying its crystallinity. While the PFS block resolidified upon transfer to 2-PrOH, the micelle struts are unlikely to have the mechanical strength of their rigid core-crystalline precursors on the template. It is possible that the mechanical integrity of the fibers is enhanced by the presence of Pt NPs embedded in the P2VP corona.⁴⁵

EDX analysis of the structures **2b** (Figure S8) showed the signals of carbon, oxygen, nitrogen, iron, silicon and platinum, similar to the element signals of **1f** (Figure S6). The curvilinear mapping of the element intensity along the scan line in the spectrum provides additional information about morphology. The EDX trace of carbon, oxygen and nitrogen of **1f** (Figure S6), where the signals were mainly contributed by the PS beads, showed a convex mapping due to the spherical shape of **1f**. After the removal of the PS core from the corona cross-linked **1c**, the EDX spectra of **2b** (Figure S8) show a concave mapping of carbon, oxygen and nitrogen signals from the micelle fibers. The concave mapping of the EDX line scan is more in accord with a collapsed hollow structure as observed in the TEM images in Figure 2a,b and Figure S7.

In summary, the hollow structures obtained here after removal of the template have some structural similarities to traditional polymersomes.^{50,51} Instead of a continuous and impermeable capsule formed by the insoluble component of these block copolymer vesicles, the outer walls of the structures formed by template removal from **1f** is composed entirely of corona cross-linked nanofiber micelles. From the lanthanide ion content of the PS beads in combination with ICP-AES measurements, we learned that there were on average 700 micelle seed crystallites anchored on each bead. In addition, we estimated the length of the micelles. If we combine this information, we would conclude that on average each basket-like structure consists of 700 interwoven and cross-linked micelles, each about $1 \mu\text{m}$ long.

Generation of Silver Nanoparticles in the Nanofibrous Membrane. Additional levels of complexity can be added to the hollow basket-like structures **2b** formed by template removal from **1f**. For example, they can serve as hosts for the incorporation of inorganic nanoparticles (NPs). In this way, one can create new hybrid structures and functions.^{52–54} We have shown in the past that partial quaternization of the

pyridine groups in the P2VP corona introduces cationic charges. In mixtures of 2-PrOH and water, these cationic sites will bind gold NPs or PbS quantum dots with negatively charged ligands at their surface.⁵⁵ Here we explore a different approach, taking advantage of the fact that use of DCM to remove the PS microbead template disrupts the crystallinity of the PFS in these structures. In the solvent-swollen state, the redox-active PFS of corona-cross-linked cylindrical PFS block copolymer micelles can generate silver nanoparticles via an *in situ* reduction of Ag⁺ ions.^{45,56}

To explore this concept, we took a sample of **2b** in DCM, purified by sedimentation–redispersion, and treated **2b** with the oxidizing agent “magic blue”. As described by Wang et al.,^{45,56} this step converts a fraction of the ferrocene (Fe(II)) groups in the PFS to ferrocenium (Fe(III)) ions. This step was followed by the addition of Ag[PF₆]. As seen in the TEM images in Figure 2c,d and Figure S9, Ag NPs (ca. 10 nm in diameter) were generated inside the corona cross-linked micelles that make up the structure. EDX analysis of the silver-encapsulated **2b** showed strong silver signals (Figure S10).

Increasing the Length of the Micelles on the Seeds@Silica@PS Microbeads. From the mechanism of CDSA for PFS block copolymers, we know that the length of the fiber-like micelles formed increases with the ratio of BCP/seeds. To examine how this affects the templated synthesis, we repeated the steps described above, adding approximately four times (0.1 mg) as much to an aliquot of a seeds@silica@PS bead (0.15 mg) sample in 2-PrOH. TEM images of the PS microbeads with the longer micelles attached to the surface before cross-linking are shown in Figure S11a,b. Here it is possible to determine the length of at least some of the protruding micelles. They appear to be uniform ($L_n = 580$ nm, $L_w/L_n = 1.04$), but much shorter than the expected length ($L_{n,expected} = 3600$ nm) calculated with eq 1. These values can be reconciled by appreciating that a significant portion of each micelle lies on the surface of the bead. The length of the protruding micelles remained unchanged after cross-linking with Pt NPs. Representative SEM and TEM images of these structures are shown in Figure S11c,d. Corresponding EDX traces are presented in Figures S12 and S13.

The cross-linked sample was suspended in DCM, subjected to several sedimentation–resuspension cycles to remove the PS template, and examined by electron microscopy. An SEM image of the resulting structure is presented in Figure 3a, with a higher magnification dark-field TEM image shown in Figure 3b and TEM images shown in Figure S14. These structures, which we refer to as **3b**, look thicker than those seen in Figure 2a,b, with a bright exterior region surrounding a darker central core. In the single structure shown in the dark-field TEM image in Figure 3b, there is a corresponding dark ring surrounding a brighter central core. Protruding fibers from the central core are prominent features of both images. These observations are consistent with collapse upon drying of hollow basket-like structures with fiber-like micelles protruding from the surface. Corresponding EDX traces are presented in Figure S15.

In Figure 3c,d and Figure S16, we show the consequences of subjecting the cross-linked hollow basket-like structures **3b** to the conditions that lead to the formation of Ag NPs. Here the Ag NPs are deposited throughout the structure (referred to as **3c**), with heavy deposition within the membrane framework of the basket, with somewhat less frequent deposition along the fibers protruding from the surface. EDX analysis of **3c** (Figure

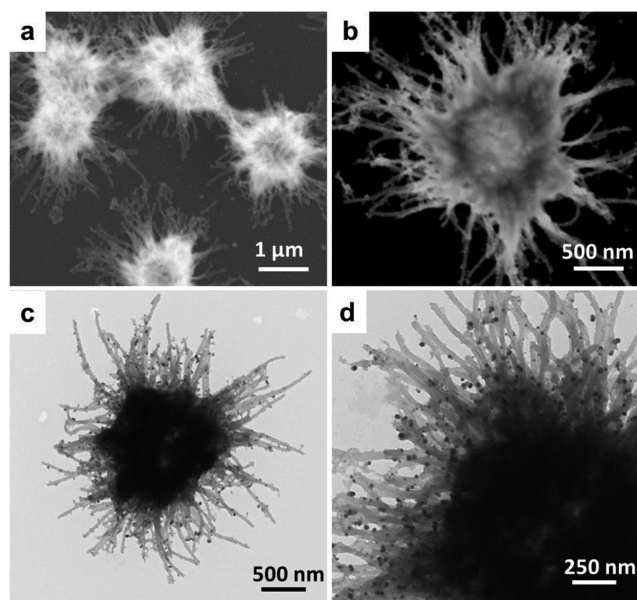


Figure 3. (a) SEM and (b) dark-field TEM images of the hollow structures obtained after cross-linking the P2VP coronae of the long protruding micelles of the PS hybrid assemblies, followed by removal of the PS template by sedimentation–resuspension in DCM. Electron microscopy images of the PS hybrid assemblies, before and after the cross-linking reaction, are presented in Figure S11. In the text and Supporting Information, the term **3b** refers to the samples whose structures are shown in (b). (c,d) TEM images of Ag NP-containing hollow structures of **3b** from different positions of the same grid at different magnifications.

S17) showed strong signals for silver as well as for the other elements (Pt, Fe, C, N) expected to be present. Elemental mapping of silver in **3c** (Figure S18) indicates that Ag NPs were embedded in the PFS-*b*-P2VP micelles. These targeted redox reactions of the ferrocene groups in the core of the hollow nanofibrous mesostructures show that there is a promising potential for this type of structure to be employed as a nanoreactor in future applications.^{57,58}

SUMMARY

In summary, we have demonstrated a new approach to fabricating colloidal nanofibrous hollow assemblies based on templated crystallization-driven self-assembly (CDSA) of core-crystalline cylindrical block copolymer micelles. In this approach, polystyrene microbeads serve as a sacrificial template. In the first step, seed crystallites of PFS₃₀-*b*-P2VP₃₀₀ BCP micelles in a selective solvent (2-PrOH) were attached to PS beads coated with a thin layer of silica. The average number of seeds per PS bead was determined by ICP-AES. Addition of more copolymer as a concentrated solution in a common good solvent (THF), led to seeded growth of fiber-like micelles from the microbead surface. If all of the seeds are active for micelle growth, then the number of seeds on the template surface determines the number and length of the micelles formed. The P2VP corona of the micelles was then cross-linked by the addition of Karstedt’s catalyst and TMDS. Vesicular assemblies were obtained after removal of the PS core by suspending the objects in DCM. These fiber-basket-like polymersomes are structurally different from the vesicles more commonly formed by amphiphilic small molecules or block copolymers. These mesostructures can be postmodified due to the presence of

pyridine groups in the corona as well as redox-active PFS in the core of the constituent micelles. We showed that partial oxidation of the ferrocene units of the PFS followed by treatment with a soluble silver salt led to deposition of silver nanoparticles along the core domain of the corona-cross-linked PFS₃₀-*b*-P2VP₃₀₀ micelles.

The templated fabrication protocol described here should in principle apply to any block copolymer that forms elongated core-crystalline micelles. For example, regioregular polylactide (e.g., PLLA) based amphiphilic block copolymers have been shown to undergo CDSA to form nanofiber-like micelles,³⁶ although conditions for seeded growth to obtain micelles of controlled length remain a challenge. If this problem can be overcome, then one could imagine preparing uniform hollow basket structures of controlled size, depending on the template, and these structures might have interesting applications as scaffolds for tissue regeneration. Additional studies are also needed to improve the quantitative determination of the structural composition of the superstructures, and to construct mechanically more robust hollow fiber-basket structures that resist collapse upon drying. In the future, by varying the number density of seeds on the template surface, one could control the number of fibers in the network and fabricate higher order structures with tailored porosity.

■ ASSOCIATED CONTENT

Supporting Information

Materials, instrumentation, and experimental details, including TEM and SEM images as well as TGA and EDX results. This material is available free of charge via the Internet at <http://pubs.acs.org>.

■ AUTHOR INFORMATION

Corresponding Authors

gguerin@chem.utoronto.ca
ian.manners@bristol.ac.uk
mwinnik@chem.utoronto.ca

Notes

The authors declare no competing financial interest.

■ ACKNOWLEDGMENTS

The authors thank the Natural Sciences Engineering Research Council of Canada for their support of this research. I.M. thanks the EU for a European Research Council (ERC) Advanced Investigator Grant. The authors would also like to thank Rachel Keunen for fruitful discussions.

■ REFERENCES

- (1) Lakes, R. *Nature* **1993**, *361*, 511.
- (2) Lafuma, A.; Quéré, D. *Nat. Mater.* **2003**, *2*, 457.
- (3) Stevens, M. M.; George, J. H. *Science* **2005**, *310*, 1135.
- (4) Glotzer, S. C.; Solomon, M. J. *Nat. Mater.* **2007**, *6*, 557.
- (5) Yan, J.; Bloom, M.; Bae, S. C.; Luijten, E.; Granick, S. *Nature* **2012**, *491*, 578.
- (6) Nie, Z.; Petukhova, A.; Kumacheva, E. *Nat. Nanotechnol.* **2010**, *5*, 15.
- (7) Pochan, D. J. *Science* **2012**, *337*, 530.
- (8) Liu, K.; Zhao, N.; Kumacheva, E. *Chem. Soc. Rev.* **2011**, *40*, 656.
- (9) Martinez-Castro, N.; Zhou, Z.; Liu, G. *Polymer* **2010**, *51*, 2629.
- (10) Hu, J.; Liu, G.; Nijkang, G. *J. Am. Chem. Soc.* **2008**, *130*, 3236.
- (11) Liu, Y.; Goebel, J.; Yin, Y. *Chem. Soc. Rev.* **2013**, *42*, 2610.
- (12) Ming, W.; Wu, D.; van Benthem, R.; de With, G. *Nano Lett.* **2005**, *5*, 2298.
- (13) Lu, Y.; McLellan, J.; Xia, Y. *Langmuir* **2004**, *20*, 3464.

- (14) Hong, J.; Han, H.; Hong, C. K.; Shim, S. E. *J. Polym. Sci., Part A: Polym. Chem.* **2008**, *46*, 2884.
- (15) Zoldesi, C. I.; Imhof, A. *Adv. Mater.* **2005**, *17*, 924.
- (16) Yi, D. K.; Lee, S. S.; Papaefthymiou, G. C.; Ying, J. Y. *Chem. Mater.* **2006**, *18*, 614.
- (17) Khanal, A.; Inoue, Y.; Yada, M.; Nakashima, K. *J. Am. Chem. Soc.* **2007**, *129*, 1534.
- (18) Zhang, M.; Zhang, W.; Wang, S. *J. Phys. Chem. C* **2010**, *114*, 15640.
- (19) Shrestha, R.; Elsbahy, M.; Luehmann, H.; Samarajeewa, S.; Florez-Malaver, S.; Lee, N. S.; Welch, M. J.; Liu, Y.; Wooley, K. L. *J. Am. Chem. Soc.* **2012**, *134*, 17362.
- (20) Elsbahy, M.; Shrestha, R.; Clark, C.; Taylor, S.; Leonard, J.; Wooley, K. L. *Nano Lett.* **2013**, *13*, 2172.
- (21) Xu, H.; Wang, W. *Angew. Chem., Int. Ed. Engl.* **2007**, *46*, 1489.
- (22) Xu, X.; Asher, S. A. *J. Am. Chem. Soc.* **2004**, *126*, 7940.
- (23) Gao, C.; Lu, Z.; Yin, Y. *Langmuir* **2011**, *27*, 12201.
- (24) Joo, J. B.; Zhang, Q.; Lee, I.; Dahl, M.; Zaera, F.; Yin, Y. *Adv. Funct. Mater.* **2012**, *22*, 166.
- (25) Zhou, J.; Zhou, M.; Caruso, R. A. *Langmuir* **2006**, *22*, 3332.
- (26) Donath, E.; Sukhorukov, G. B.; Caruso, F.; Davis, S. A.; Möhwald, H. *Angew. Chem., Int. Ed.* **1998**, *37*, 2201.
- (27) Niu, Z.; Liu, J.; Lee, L. A.; Bruckman, M. A.; Zhao, D.; Koley, G.; Wang, Q. *Nano Lett.* **2007**, *7*, 3729.
- (28) Jiang, N.; Xu, Y.; He, N.; Chen, J.; Deng, Y.; Yuan, C.; Han, G.; Dai, L. *J. Mater. Chem.* **2010**, *20*, 10847.
- (29) Wu, Q.; Wang, Z.; Xue, G. *Adv. Funct. Mater.* **2007**, *17*, 1784.
- (30) Liu, X.; Jin, X.; Ma, P. X. *Nat. Mater.* **2011**, *10*, 398.
- (31) Jia, L.; Zhao, G.; Shi, W.; Coombs, N.; Gourevich, I.; Walker, G. C.; Guerin, G.; Manners, I.; Winnik, M. A. *Nat. Commun.* **2014**, *5*, 3882.
- (32) Wang, X.; Guerin, G.; Wang, H.; Wang, Y.; Manners, I.; Winnik, M. A. *Science* **2007**, *317*, 644.
- (33) He, F.; Gädt, T.; Jones, M.; Scholes, G. D.; Manners, I.; Winnik, M. A. *Macromolecules* **2009**, *42*, 7953.
- (34) Jeong, N. S.; Manners, I. *Macromol. Chem. Phys.* **2009**, *210*, 1080.
- (35) Schmelz, J.; Schedl, A. E.; Steinlein, C.; Manners, I.; Schmalz, H. *J. Am. Chem. Soc.* **2012**, *134*, 14217.
- (36) Petzetakis, N.; Dove, A. P.; O'Reilly, R. K. *Chem. Sci.* **2011**, *2*, 955.
- (37) He, W.-N.; Xu, J.-T.; Du, B.-Y.; Fan, Z.-Q.; Wang, X. *Macromol. Chem. Phys.* **2010**, *211*, 1909.
- (38) Qian, J.; Li, X.; Lunn, D. J.; Gwyther, J.; Hudson, Z. M.; Kynaston, E. M.; Rugar, P. A.; Winnik, M. A.; Manners, I. *J. Am. Chem. Soc.* **2014**, *136*, 4121.
- (39) Kamps, A. C.; Fryd, M.; Park, S.-J. *ACS Nano* **2012**, *6*, 2844.
- (40) Lee, E.; Hammer, B.; Kim, J.-K.; Page, Z.; Emrick, T.; Hayward, R. C. *J. Am. Chem. Soc.* **2011**, *133*, 10390.
- (41) Liang, Y.; Abdelrahman, A. I.; Baranov, V.; Winnik, M. A. *Polymer* **2011**, *52*, 5040.
- (42) Liang, Y.; Abdelrahman, A. I.; Baranov, V.; Winnik, M. A. *Polymer* **2012**, *53*, 998.
- (43) Goodwin, J. W.; Hearn, J.; Ho, C. C.; Ottewill, R. H. *Colloid Polym. Sci.* **1974**, *252*, 464.
- (44) Shen, L.; Wang, H.; Guerin, G.; Wu, C.; Manners, I.; Winnik, M. A. *Macromolecules* **2008**, *41*, 4380.
- (45) Qiu, H.; Du, V. A.; Winnik, M. A.; Manners, I. *J. Am. Chem. Soc.* **2013**, *135*, 17739.
- (46) In the absence of cross-linking, the PFS-*b*-P2VP micelles as well as the PS beads dissolved in dichloromethane.
- (47) Liu, X.; Jiang, M. *Angew. Chem., Int. Ed. Engl.* **2006**, *45*, 3846.
- (48) Wang, J.; Jiang, M. *J. Am. Chem. Soc.* **2006**, *128*, 3703.
- (49) Liu, F.; Eisenberg, A. *J. Am. Chem. Soc.* **2003**, *125*, 15059.
- (50) Discher, B. M.; Won, Y. Y.; Ege, D. S.; Lee, J. C.; Bates, F. S.; Discher, D. E.; Hammer, D. A. *Science* **1999**, *284*, 1143.
- (51) Jia, L.; Lévy, D.; Durand, D.; Impéror-Clerc, M.; Cao, A.; Li, M.-H. *Soft Matter* **2011**, *7*, 7395.

- (52) Franke, T.; Schmid, L.; Weitz, D. A.; Wixforth, A. *Lab Chip* **2009**, *9*, 2831.
- (53) Li, G. L.; Xu, L. Q.; Neoh, K. G.; Kang, E. T. *Macromolecules* **2011**, *44*, 2365.
- (54) Schulz, M.; Olubummo, A.; Binder, W. H. *Soft Matter* **2012**, *8*, 4849.
- (55) Wang, H.; Lin, W.; Fritz, K. P.; Scholes, G. D.; Winnik, M. A.; Manners, I. *J. Am. Chem. Soc.* **2007**, *129*, 12924.
- (56) Wang, H.; Wang, X.; Winnik, M. A.; Manners, I. *J. Am. Chem. Soc.* **2008**, *130*, 12921.
- (57) Ding, S.; Chen, J. S.; Qi, G.; Duan, X.; Wang, Z.; Giannelis, E. P.; Archer, L. A.; Lou, X. W. *J. Am. Chem. Soc.* **2011**, *133*, 21.
- (58) Vriezema, D. M.; Comellas Aragonès, M.; Elemans, J. A. A. W.; Cornelissen, J. J. L. M.; Rowan, A. E.; Nolte, R. J. M. *Chem. Rev.* **2005**, *105*, 1445.